



Degradation of diazinon from aqueous solution using silver-modified clinoptilolite zeolite in photocatalytic process

Milad Hallajiqomi, Mohsen Mehdipourghazi*, Farshad Varaminian

Faculty of Chemical, Petroleum and Gas Engineering, Semnan University, Semnan, Iran

ARTICLE INFO

Article history:

Received 10 August 2018

Received in revised form

3 March 2019

Accepted 9 March 2019

Keywords:

Clinoptilolite Zeolite-Silver

Diazinon

Microwave Irradiation

Photocatalytic Degradation

Photocatalytic Reactor

ABSTRACT

photocatalytic reactor was tested in the degradation of diazinon in water using photocatalyst clinoptilolite zeolite-silver. The photocatalyst clinoptilolite zeolite-silver was synthesized using a microwave energy technique. The influence of AgO in the photocatalytic reactor was investigated for diazinon treatment. The prepared photocatalyst was authenticated by X-Ray Diffraction (XRD), for Field Emission Scanning Electron Microscope (FESEM), Brunner-Emmet-Teller (BET), and Diffuse Reflectance Spectroscopy (DRS) analysis methods. Every one of the mixtures was analyzed using XRD, and the three distinctive peaks ($2\theta = 9.84, 11.17, \text{ and } 22.35$) of clinoptilolite were chosen for which the calculations of the peak intensity summation were done. The experiments appraised the influence of various empirical factors, e.g., pH, photocatalyst dosage, initial diazinon, and irradiation time on the degradation efficiency. The results showed that the optimum conditions for diazinon degradation were a pH of 9, photocatalyst dosage of 1 g/L and irradiation time of 120 min. The point of zero charge (pzc) of the photocatalyst clinoptilolite zeolite-silver, the point when the surface charge density is zero, was identified to be 8. This excellent catalytic ability was mainly attributed to the hybrid effect of the photocatalyst and adsorbent.

1. Introduction

Nowadays a wide range of pesticides is used in agriculture and horticulture that include different types of insecticides, fungicide, herbicide, nematicide, acaricide, etc. These chemicals have become a threat to the environment because they are being released into water and soil from industrial sewage and agricultural runoffs. Animals such as bees, birds, and aquatic animals have the highest degree of exposure to pesticides and are severely threatened by them. Moreover, pesticides are formulated with chemicals such as phosphorous, sulfur and chlorine which pose a threat for the eco-system, as well as being hazardous for humans [1]. In previous researches, various methods have been proposed to remove these pharmaceutical components from water or wastewater flows. Two of these approaches include ultrasound and ozonation. Other methods like Fenton or photo-Fenton systems are included among the proposed techniques for purifying water. The

process of adsorbing the pollutants with activated carbon is also listed among them, and reverse osmosis is considered a reliable approach. In the previous researches it has been proposed to utilize the method of photolysis with hydrogen peroxide ($\text{UV}/\text{H}_2\text{O}_2$). Advanced oxidation processes (AOPs) have been developed in recent times and include the photocatalytic process. AOPs are considered to be one of the best methods in case of efficiency for aqueous environment treatment. These photocatalytic processes utilize the hydroxyl radicals (OH) that are produced by reacting with a wide range of pollutants in water and wastewater flows; this results in their disintegration into CO_2 and H_2O [1-3]. Zeolites are microporous crystalline hydrated aluminosilicates which can structurally be considered as inorganic polymers built from an infinitely extending three-dimensional network of tetrahedral TO_4 units, where T is Si or Al. Each aluminum ion that is present in the zeolite framework yields a net negative charge, which is balanced by an extra framework cation, usually from

*Corresponding author. Tel: +98 2331533922

E-mail address: mohsenmehdipour@semnan.ac.ir

DOI: 10.22104/aet.2019.3010.1147

group IA or IIA. The zeolite framework structure contains channels or interconnected voids of discrete size (in the range of 3–20 Å) occupied by the charge balancing ions and water molecules [3–5]. Applying other methods for heating (e.g., microwave irradiation) significantly improves the synthesis of clinoptilolite zeolite. In recent years, the use of dielectric heating has resulted in a higher rate of efficiency in the synthesis of zeolite; this occurs because the three factors in the zeolite synthesis decrease. These factors include crystal growth, nucleation, and the induction period [6]. Although microwave energy is an efficient source for heating, it has not been significantly analyzed in the field of synthesizing zeolite [7]. Also, the microwave equipment and synthesis factors are not often indicated in the researches. These actors include mixture volume, composition, pressure and temperature [8]. Moreover, the morphology of the zeolite crystal and also the distribution of the size are not always reported. The absence of this data hinders the profound understanding of the synthesis of the molecular sieves when applying microwave irradiation [7–9]. In this research, the presence of the photocatalyst clinoptilolite zeolite-silver (CP/Ag) in a feed on the process performance was investigated. This work used a novel photocatalyst CP/Ag synthesis using a microwave energy technique. The particles of zeolite were used to obtain clinoptilolite/Ag as a heterogeneous catalyst for the degradation of diazinon in an aqueous solution under visible light via a simple method. Clinoptilolite zeolite (CP) was the adsorbent of choice due to its good adsorption properties and availability at an affordable cost. The research investigated the impacts that the initial diazinon concentration, irradiation time, photocatalyst amount, and pH have on the efficiency of the degradation. The as-prepared samples were characterized by X-Ray Diffraction (XRD), Field Emission Scanning Electron Microscope (FE-SEM, Mira 3-XMU, TESCAN Company), Brunner-Emmet-Teller method (BET, Belsorpmini II Japan), UV-Vis spectrophotometer (Avantes, Avaspec-2048-TEC), and Diffuse Reflection Spectroscopy (DRS).

2. Materials and methods

2.1. Materials

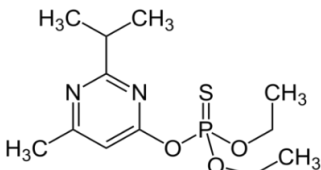
The materials used in this work included silver nitrate (AgNO_3), sodium hydroxides (NaOH), potassium hydroxides (KOH), tetraethylorthosilicate ($\text{SiC}_8\text{H}_{20}\text{O}_4$) (TEOS), aluminum hydroxide ($\text{Al}(\text{OH})_3$), acetone ($(\text{CH}_3)_2\text{CO}$) and sulfuric acid, which were all obtained from the Merck Company. The technical grade of the insecticide diazinon (>95%) (Shown in the structure in Table 1) was supplied from Chem-service (USA). In the research, all the materials except for deionized water were applied without changing their initial condition.

2.2. Synthesis of Photocatalyst Clinoptilolite Zeolite-Silver

The silver (Ag) modification of clinoptilolite (CP) zeolite was achieved by shaking 20 g of clinoptilolite zeolite in 500 mL of 3% (w/v) AgNO_3 ; then, it was kept at 60 °C for 24 h with

magnetic stirring. The silver modified clinoptilolite zeolite (CP/Ag) was separated from the solution by filtration and washed with deionized water. It was dried overnight at 100 °C for 24 h and then calcined at 300 °C for 5 h. Since this compound was synthesized in a low-temperature deposition method, it was in an amorphous state. Therefore, in order to obtain crystalline products, it was necessary to conduct secondary thermal processes such as calcination. The samples were then transferred to vials and stored in the dark because exposure to light decreases their photocatalytic properties.

Table 1. Chemical structure and characteristics of diazinon [6].

Chemical structure	
	
Molecular formula	$\text{C}_{12}\text{H}_{21}\text{N}_2\text{O}_3\text{PS}$
Mw (g/mol)	304.3
λ_{max} (nm)	247
solubility in water in 25°C(mg/L)	40
Flash point (°C)	82

2.3. Photocatalytic degradation experiments

A photocatalytic reactor with two lamps (Philips, 120W) was used as the visible irradiation source to degrade the diazinon. With the purpose of producing the diazinon solution, the contents of an effective material were dissolved in water and shaken for 45 min; then, it was filtered in a 10000 mL volumetric flask and diluted with water. The photoreactor was filled with 3000 ml of 25 mg/L pollutant and 0.5 g/L of photocatalyst at an irradiation time of 120 min. The whole reactor was cooled on its outside with a water-cooled jacket. The temperature was maintained at 26 °C. With the purpose of allowing the diazinon molecules to absorb on the CP/Ag surface and before photodecomposition, the solution which contained a fixed amount of the photocatalyst was blended for 30min in the absence of any light. In order to set the adsorption/desorption equilibrium of the pollutant on a heterogeneous catalysts surface, the reactor was kept under dark conditions for 45 min. An aliquot suspension was withdrawn and centrifuged at 6000 rpm to remove the solid particles. The UV–V is the absorption spectra of the diazinon solution, which was scanned and showed an optimum band centered at 247 nm. It can be utilized as the absorbance wavelength for the formation of the diazinon standard curve based on the Lambert-Beer law. The standard curve can be utilized to quantify the concentrations of different diazinon samples. The degree of degradation was calculated

by the following formula, which is based on the absorbance of the solution (at $\lambda_{\max}=247$ nm) before and after irradiation.

$$\text{diazinon degradation \%} = [(C_0 - C_t)/C_0] * 100 = [(A_0 - A_t)/A_0] * 100 \quad (1)$$

where C_0 and C_t are the initial and final concentration of diazinon at time t , respectively. A_0 and A_t are respectively the initial and final absorbance of the samples. The absorbance values were used to calculate the percent of degradation.

3. Results and discussion

3.1. Characterization of products by XRD

Figure 1 shows the XRD pattern of the CP zeolite collected at the bottom of the autoclave. XRD analyses were performed for each mixture, and the peak intensity summation was calculated for the three characteristic peaks ($2\theta=9.84, 11.17, 22.35$) of clinoptilolite. One of the products, BC 4, which was synthesized in this study and has the highest intensity summation, was selected as 100% clinoptilolite. The comparative XRD spectra of the synthesized CP zeolite and the Ag-doped zeolite (CP/Ag) are presented in Figure 1. The thermal treatment of Ag-doped

zeolite caused the intensities of reflection observed at about $8.7^\circ, 10.45^\circ,$ and 21.95° relating to the quantity of clinoptilolite to reduce [10]. The presence of a low amount of silver in the zeolite showed no significant difference in the patterns of diffraction. Nevertheless, traces of AgAlO_2 ($26.19^\circ; 31.58^\circ$) were identified.

3.2. Morphology of products by FE-SEM

Figure 2 presents the FE-SEM image of the clinoptilolite zeolite that was thermally treated and Ag-doped. Figure 2 shows the considerable changes in the morphology of the Ag-doped zeolite in correlation with the synthesized clinoptilolite zeolite. Some small particles which were agglomerated on the zeolitic material were observed [11]. The metallic Ag particles were observed to be distributing homogeneously on the surface of the zeolite cluster. The agglomeration of more silver particles on the surface of the Ag-zeolite composite may have caused the composite cluster size to become larger. Moreover, another reason for the increase in the cluster size of the CP/Ag composites could be the nucleation and growth of the metallic Ag inside the zeolite internal pores [12].

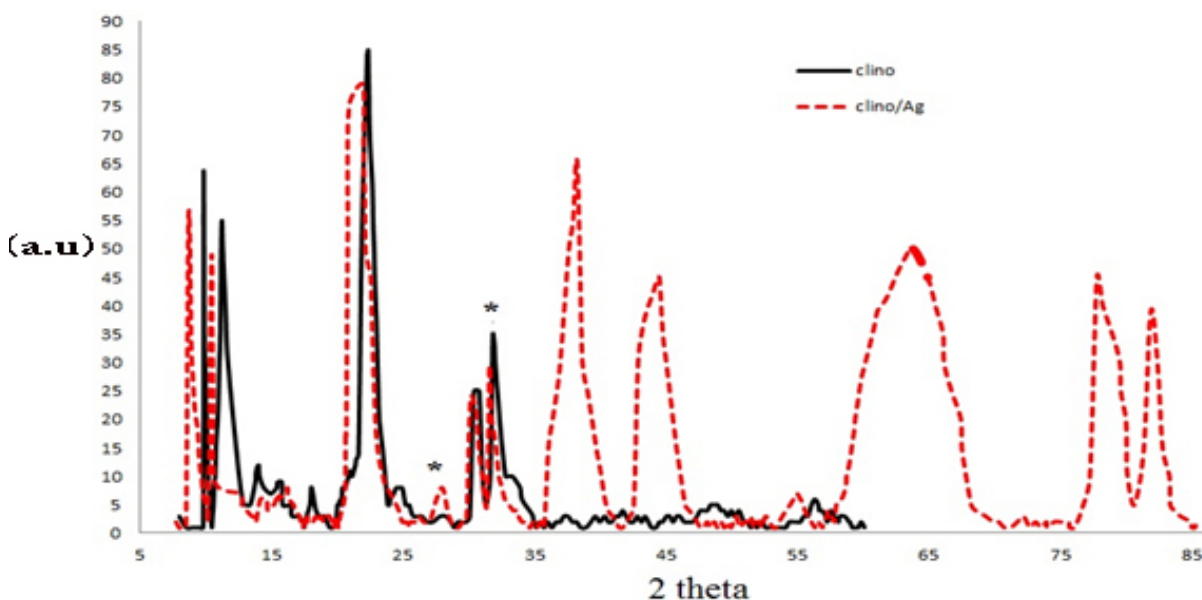


Fig. 1. X-ray diffraction data of synthetic clinoptilolite zeolite and g-doped clinoptilolite zeolite.

3.3. BET surface area analysis

The surface area (S_{BET}) of the samples was determined from the N_2 adsorption-desorption isotherms using the Brunner-Emmet-Teller method. The surface area of BET for the prepared photocatalysts is shown in Table 2. In a different research [11-13], the surface area and average pore diameter of the different percentages of AgO on the zeolite were observed. The surface texture properties of the raw clinoptilolite (CP), Ag supported clinoptilolite (CP/Ag)

samples were determined by N_2 adsorption and the obtained results are summarized in Table 2. As shown, because of the possible blocking of some zeolite pores by the Ag, the Ag semiconductor by clinoptilolite reduces the surface area and also the total pore volume. The formation of Ag in the zeolite channels and surface causes the solid particle size to get larger and the surface area and pore volume to become smaller [13-14].

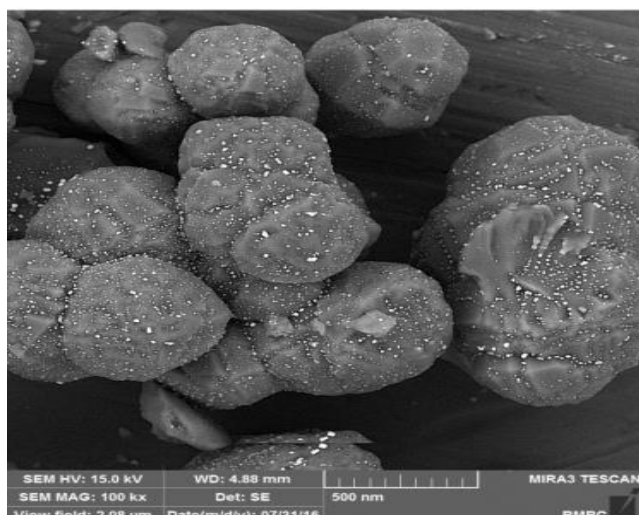


Fig. 2. FE-SEM image of Ag-doped synthetic clinoptilolite zeolite.

Table 2. BET surface area results for various prepared samples.

Sample	S _{BET} (m ² /g)	V _p (cm ³ /g)	d _p (nm)	Constant C
AgO	23.81	2.42	28	32.8
(CP)	235.93	5.95	26.74	1011.8
CP/Ag	167.24	4.05	45.88	253.85

3.4. DRS studies

The UV-vis diffuse reflectance spectroscopy (DRS) was applied to investigate the optical characteristics of the catalyst and is presented in Figure 3. Clearly, the CP/Ag catalyst was able to absorb both the UV and visible light well. It could be seen that the CP/Ag sample showed absorbance in the visible range, which suggested its potential to be activated by visible light. Using the UV-vis spectra to determine the band gap was an alternative approach to investigate the modification of the electronic property of the synthesized species. The energy band structure was a key factor affecting the photo catalytic activity of the catalysts [15]. According to the definitions in physics, if there is an energy range in the solid in which none of the electrons can have an existing state, that range can be called a band gap. For example, in semiconductors, if the energy difference that exists from the valence's top to the conduction band's bottom is measured, this amount can be related to the band gap. This actually is the exact amount of energy that is sufficient in order to take a valence electron bound higher in an atom, and therefore, the so-called electron will be a conduction electron. This electron can then transfer inside the crystal lattice very freely. Thus, these transferring electrons can be the charge carrier, which means they can transfer electricity. But in some situations, the so-called electrons are not able to transfer. These situations consist of two conditions. One is that the valence band is totally full, and the other is that the conduction band is totally empty. On the other hand, an electric current can occur in a situation where there are electrons which can

move from the valence to the conduction band. Thus, the band gap is the main parameter for determining the electrical conductivity of a solid [15-18].

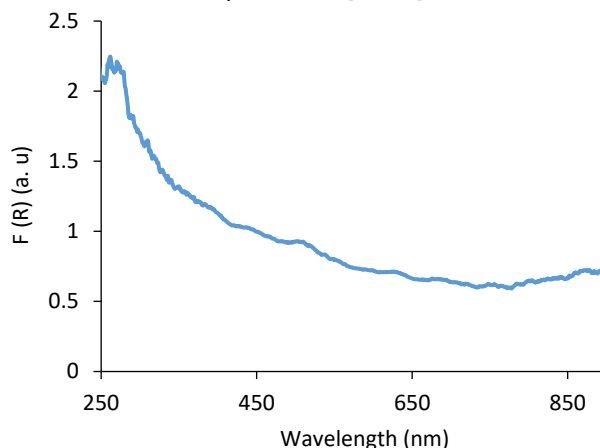


Fig. 3. UV-Vis diffuse reflectance spectra of commercial Ag-doped clinoptilolite zeolite sample.

Tauc's equation estimates the band gap of the composite by applying the absorption data [16]:

$$\alpha = \alpha_0 (h\nu - E_g)^n / h\nu \quad (2)$$

where represents the coefficient of absorption, h and α_0 are the constants, $h\nu$ represents the energy of the photon, E_g pertains the material's optical band gap, and n is dependent on the electronic transition type that has a value between 0.5 and 3. The extrapolation of the linear portion of the plots of $(\alpha h\nu)^{0.5}$ against $h\nu$ to the energy axis was done to recognize the sample's energy gap (E_g). The following formula can determine the valence band (V_B) and conduction band (C_B) potentials of the semiconductor at the point of zero charge:

$$E_{VB} = X - E_c + 0.5 E_g \quad (3)$$

where E_{VB} or E_{CB} represent the V_B or C_B edge potentials of the semiconductor, X pertains to the absolute electronegativity of its constituent atoms, E_c stands for the free electrons' energy on the hydrogen scale (ca. 4.5 eV), and E_g represents the band gap of the semiconductor. The C_B position can be calculated by $E_{CB} = E_{VB} - E_g$ [16]. Since the zeolites generally do not absorb any light in UV-vis regions, they are one of the most suitable supports for photocatalysis. The results revealed a clear trend in decreasing the band gap of commercial AgO to 2.47 eV for Ag supported on CP. This suggested that the particle size of the AgO supported on the zeolite was larger than that of the commercial AgO which was used in the present study (quantum size effect) [17-18]. Furthermore, the zeolite delocalized the band-gap excited electrons of Ag, and therefore minimized the electron/hole recombination.

3.5. Photo-degradation mechanism

The proposed mechanism of photo catalytic performance, photo excitation, and charge transfer in the CP/AgO under

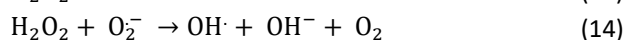
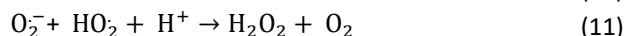
visible light irradiation is shown in Figure 4. Under visible light irradiation, the AgO shows no photo electronic response due to the wide band gap (2.47 eV), while both the Ag and AgO nanoparticles are excited and produced h^+ and e^- as cited in the following formula:



We proposed that the trapped electrons could be transferred to the oxygen on the nanocomposite surface and produce a superoxide radical, or it could be further reacted with AgO and reduce it to Ag.



The generated anion superoxide and the holes in the AgO react with the adsorbed H_2O on the surface of the nanocomposite and produce an active OH^\bullet species. It is assumed that the generated hydrogen peroxide converted to an OH^\bullet species with three possible reactions.



Diazinon can be oxidized by the trapped holes on the AgO nanoparticles or the free reactive OH^\bullet species in the solution and decomposed to carbon dioxide, water and other inorganic components.

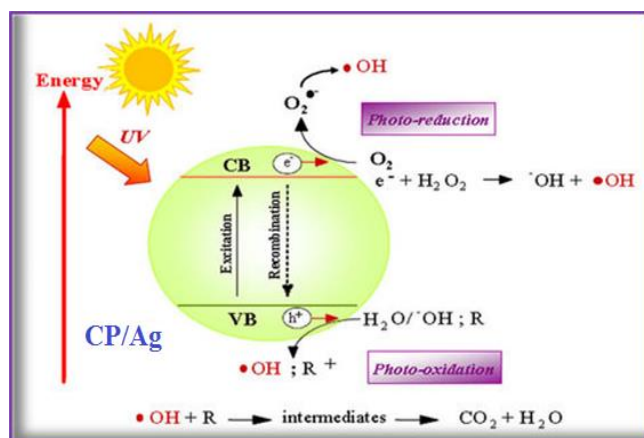
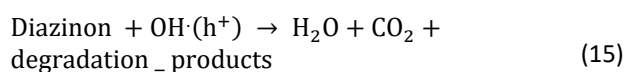


Fig. 4. Schematic view of proposed charge transfer mechanism of CP/Ag photocatalyst under visible light radiation.

3.6. Effect of Irradiation time

As illustrated in Table 3, time is an important parameter which directly affects the degradation efficiency. Table 3 shows the experimental runs that measure the effect of the

irradiation time of a 50 mL of diazinon solution with an initial concentration of 25 mg/L in distilled water that was treated with 1000 mg of CP/Ag nanophotocatalyst at 26°C at a pH value of 8 with an irradiation time increment from 30 min to 90 min. The outcome showed that the degradation of diazinon was quick and only after 120 minutes of irradiation; the condition of equilibrium was reached.

Table 3. Effect of irradiation time in diazinon degradation.

Type of photocatalyst	Irradiation time (min)	Initial conc. (mg/L)	Degradation efficiency (%)
CP/Ag	30	25	42±1
	45	25	67±1
	60	25	75±1
	75	25	89±1
	90	25	95±1

3.7. Effect of pH

The pH of the aqueous solution was a major factor in controlling the process of degradation. With the aim of investigating the impact of pH on the efficiency of the diazinon degradation, 50 mL of TC solution, which had the initial concentration of 25 mg/L in distilled water, was treated with 500 mg of CP/Ag nanophotocatalyst and 500 mg of CP at different pH values. The results are summarized in Table 4. It was concluded that the degradation of diazinon by applying the CP/Ag photocatalyst was highly dependent on the pH.

Table 4. Effect of pH in diazinon degradation.

No.	Type of photocatalyst	pH	Initial conc. (mg/L)	Degradation efficiency (%)
1	CP/Ag	4±0.1	25	29±1
2	CP/Ag	5±0.1	25	41±1
3	CP/Ag	6±0.1	25	58±1
4	CP/Ag	7±0.1	25	73±1
5	CP/Ag	8±0.1	25	95±1
6	CP/Ag	9±0.1	25	87±1

The point of the zero charge (pzc) of the photocatalyst clinoptilolite zeolite-silver when the surface charge density is zero was found to be 8; it is shown in Figure 5. This value corresponded to the pH at which the straight line ($\text{pH}_{\text{initial}} = \text{pH}_{\text{final}}$) crossed the sigmoid curve passing through the experimental points [19]. The electric charge properties of both the catalyst and substrate were found to play an important role in the adsorption process. The surface of the catalyst was positively charged at a $\text{pH} < \text{pH}_{\text{pzc}}$, negatively charged at a $\text{pH} > \text{pH}_{\text{pzc}}$, and remained neutral at a $\text{pH} =$

pH_{PZC} . Such behavior significantly affected not only the adsorption-desorption properties of the catalyst surface but also the changes of the pollutant structure at various pH values.

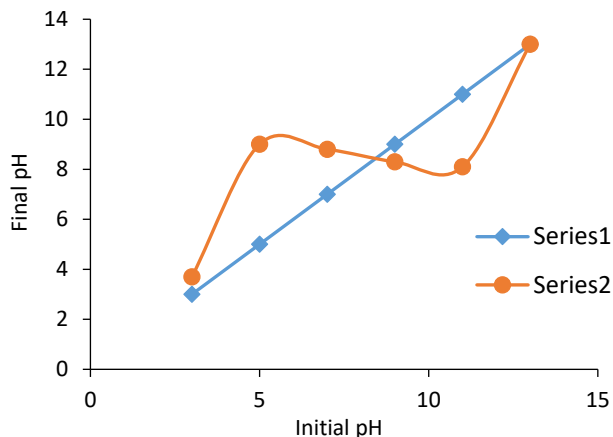


Fig 5. pH_{PZC} of photocatalyst clinoptilolite zeolite-silver (Series 1: Standard, Series 2: Synthesized photocatalyst).

3.8. Effect of photocatalyst dosage on the degradation efficiency

The effect of the photocatalysts clinoptilolite zeolite-silver and clinoptilolite zeolite on pollutant degradation was analyzed when their concentration was between 0.25–1.5 g/L through the constant initial diazinon concentration of 25 mg/L at pH 8. As shown in Figure 6, increasing the concentration of the catalyst enhanced the efficiency of the degradation; this was caused by the increase in the surface area or the sites that were activated. Nevertheless, it is noteworthy that the addition of more amounts of catalyst can change the process of degradation in a way that it is less efficient. The increase in the scattering and turbidity effects was actually related to that because it inhibited the penetration of light into all the particles' surfaces [20-22].

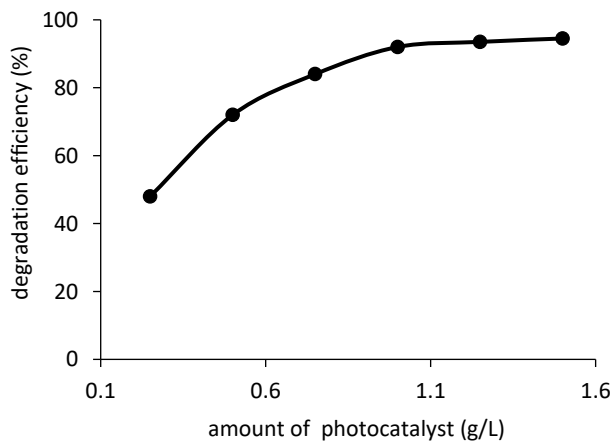


Fig 6. The effect of photocatalyst dosage on degradation efficiency of diazinon: pH, 8; initial concentration, 25 mg/L; irradiation time, 90 minutes at 26 °C

3.9. Effect of Diazinon initial concentration

The change in the inlet concentrations of the contaminant causes the rates of the reaction to change. According to Figure 7, the efficiency of the degradation is reduced at the time that the initial diazinon concentration becomes greater, and this behavior has some causes. The quantity of the diazinon particles that are attracted to the active surface of the photocatalyst increases at the time that the initial concentration of the pollutant becomes greater. In this situation, the pH, the catalyst dosage and the time of the reaction are maintained at the same value; thus, the quantity of the reactive species ($^{\circ}\text{OH}$ and $^{\circ}\text{O}^{-2}$) does not change. As a result, the current reactive radicals are not sufficient for concentrations of diazinon that are high. Moreover, at the time that the concentration of the substrate is reduced, the production of intermediate scan occur and diffuse in the surface of the photocatalyst, which leads to deactivation of the reaction sites [23-25]. Therefore, the results show that with an increase in the initial concentration of the diazinon, the amount of catalyst surface that is sufficient for the degradation increases. It is possible that this happens because of the shifting in the regime. The initial situation of the change is the condition in low concentrations, where there is a kinetic control regime. Then, the system changes to some extent at high concentrations. When photocatalytic oxidation occurs, the concentration of the organic substrate is affected by the photonic efficiency. When the concentrations of the substrate increase, there is a decrease in the photonic efficiency. Also, the surface of the photocatalyst is filled, and this results in the deactivation of the catalyst [25].

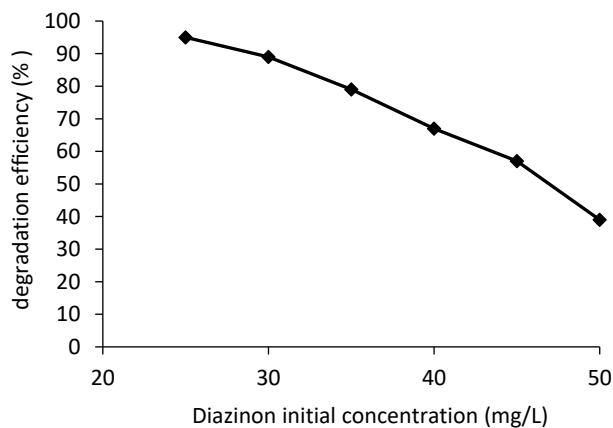


Fig 7. The effect of diazinon initial concentration on degradation efficiency of diazinon: pH, 8; photocatalyst concentration, 0.5 g/L; irradiation time, 90 minutes at 26 °C

3.10. Photocatalytic degradation kinetics

In order to investigate the kinetic behavior of photocatalytic degradation, diazinon with different photo reduction time irradiated photocatalysts was chosen to prepare the CP/Ag photocatalysts for the degradation of diazinon under visible light irradiation. The Langmuir-Hinshelwood kinetic

equation is usually used to describe the photocatalytic heterogeneous surface reactions, where the reaction rate is calculated by the following equation [26-29]:

$$\frac{dC_t}{dt} = K \frac{K_{TC} C_t}{1 + K_{TC} C_0} \quad (16)$$

Where K is the Langmuir Hinshelwood adsorption coefficient (L/mg), K_{TC} is the reaction rate constant ($\text{mgL}^{-1}\text{min}^{-1}$), C_t and C_0 are denoted to the tetracycline concentration of the initial and reaction time t. If the initial concentration used is sufficiently small ($<10^{-3}\text{mol/L}$), the simplification of this kinetic equation into a pseudo first-order equation is frequently employed, which can be given by the following equation:

$$\ln\left(\frac{C_t}{C_0}\right) = Kt \quad (17)$$

where K denotes to the pseudo-first-order rate constant (min^{-1}), which has been cited to be appropriate for the comparison of different photocatalytic systems as it is independent of the concentration and regards the calculation of photocatalytic activity independent of the dark adsorption. Figure 8 describes the liner relationship between the $\ln(C_t/C_0)$ and reaction time t, where the slopes of the lines represent the pseudo-first-order rate constant. The results are shown in Table 5.

Table 5. Kinetics parameters for photocatalytic degradation of diazinon.

Type of photocatalyst	Equation	K(min^{-1})	$t_{1/2}$ (min)	(R^2)
CP/Ag	$y = 0.0215x - 0.072$	0.0215	54	0.994

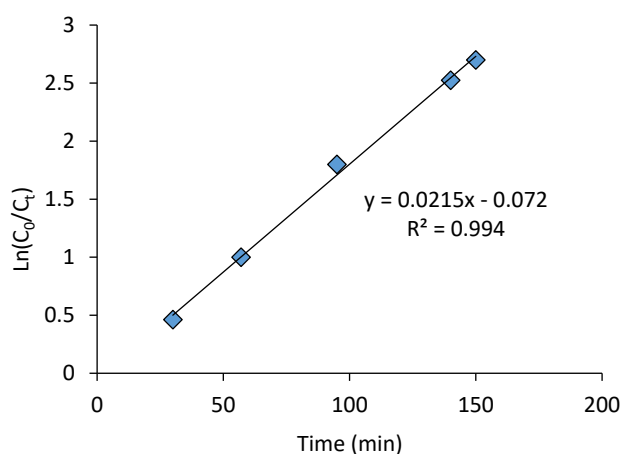


Fig. 8. The pseudo first-kinetic of photocatalytic degradation diazinon with CP/Ag photocatalyst.

4. Conclusions

In summary, zeolite clinoptilolite and its nanocomposite clinoptilolite zeolite-silver were successfully synthesized by microwave irradiation and applied as the photocatalyst for the degradation of diazinon in water. The results of this

study suggested that the surface immobilization of AgO onto CP could enhance its surface area and its ability to activate under visible light. The specific surface area for the composited material reached $167\text{m}^2/\text{g}$, which was eight times larger than the unmodified AgO. The photocatalytic activities of the catalysts were studied by measuring the photo degradation of the diazinon solution. The degradation of diazinon via the CP/Ag nano photo catalyst was found to be a strongly pH-dependent process. The catalysts showed a pH dependence, and more than 95% of the diazinon could be removed from the solution within 90 min at a pH of 8. Also, the degradation efficiency was developed with increments of catalyst concentration. The finding of this study could benefit future applications in water and wastewater treatment. A very important advantage of the photocatalytic processes presented here is the complete separation of the catalyst particles, as well as the dye and other non-volatile compounds.

References

- [1] Ahmed, S., Rasul, M. G., Brown, R., Hashib, M. A. (2011). Influence of parameters on the heterogeneous photocatalytic degradation of pesticides and phenolic contaminants in wastewater: a short review. *Journal of environmental management*, 92(3), 311-330.
- [2] Collazzo, G. C., Foletto, E. L., Jahn, S. L., Villetti, M. A. (2012). Degradation of Direct Black 38 dye under visible light and sunlight irradiation by N-doped anatase TiO_2 as photocatalyst. *Journal of environmental management*, 98, 107-111.
- [3] Meier, W. M. (1996). Atlas of zeolite structure types. *Zeolites, Special issue*, 17.
- [4] Stolz, J., Yang, P., Armbruster, T. (2000). Cd-exchanged heulandite: symmetry lowering and site preference. *Microporous and Mesoporous Materials*, 37(1-2), 233-242.
- [5] Mohammadi, A., Aliakbarzadeh Karimi, A. (2017). Methylene blue removal using surface-modified TiO_2 nanoparticles: A comparative study on adsorption and photocatalytic degradation. *Journal of Water and Environmental nanotechnology*, 2(2), 118-128.
- [6] Moslehiani, A., Ismail, A. F., Othman, M. H. D., Matsuura, T. (2015). Hydrocarbon degradation and separation of bilge water via a novel TiO_2 -HNTs/PVDF-based photocatalytic membrane reactor (PMR). *RSC Advances*, 5(19), 14147-14155.
- [7] Hairom, N. H. H., Mohammad, A. W., Kadhun, A. A. H. (2015). Influence of zinc oxide nanoparticles in the nanofiltration of hazardous Congo red dyes. *Chemical engineering journal*, 260, 907-915.
- [8] Shiohawa, K., Ito, M., Itabashi, K. (1989). Crystal structure of synthetic mordenites. *Zeolites*, 9(3), 170-176.
- [9] Balou, J., Khalilzadeh, M. A., Zareyee, D. (2017). KF/Nano-clinoptilolite Catalyzed Aldol-Type Reaction

- of Aldehydes with Ethyl Diazoacetate. *Catalysis letters*, 147(10), 2612-2618.
- [10] Jury, F. A., Polaert, I., Estel, L., Pierella, L. B. (2014). Enhancement of synthesis of ZSM-11 zeolite by microwave irradiation. *Microporous and mesoporous materials*, 198, 22-28.
- [11] Morones, J. R., Elechiguerra, J. L., Camacho, A., Holt, K., Kouri, J. B., Ramírez, J. T., Yacaman, M. J. (2005). The bactericidal effect of silver nanoparticles. *Nanotechnology*, 16(10), 2346.
- [12] Yamanaka, M., Hara, K., Kudo, J. (2005). Bactericidal actions of a silver ion solution on Escherichia coli, studied by energy-filtering transmission electron microscopy and proteomic analysis. *Applied and environmental microbiology*, 71(11), 7589-7593.
- [13] Mahmoodi, P., Hosseinzadeh Borazjani, H., Farhadian, M., Solaimany Nazar, A. R. (2015). Remediation of contaminated water from nitrate and diazinon by nanofiltration process. *Desalination and water treatment*, 53(11), 2948-2953.
- [14] Rivera-Garza, M., Olguin, M. T., Garcia-Sosa, I., Alcántara, D., Rodriguez-Fuentes, G. (2000). Silver supported on natural Mexican zeolite as an antibacterial material. *Microporous and mesoporous materials*, 39(3), 431-444.
- [15] Kusvuran, E., Yildirim, D., Mavruk, F., Ceyhan, M. (2012). Removal of chloropyrifos ethyl, tetradifon and chlorothalonil pesticide residues from citrus by using ozone. *Journal of hazardous materials*, 241, 287-300.
- [16] Sheng, J., Tong, H., Xu, H., Tang, C. (2016). Preparation and Photocatalytic Activity of SnO₂@ TiO₂ Core-Shell Composites Modified by Ag. *Catalysis surveys from Asia*, 20(3), 167-172.
- [17] Krishnani, K. K., Zhang, Y., Xiong, L., Yan, Y., Boopathy, R., Mulchandani, A. (2012). Bactericidal and ammonia removal activity of silver ion-exchanged zeolite. *Bioresource technology*, 117, 86-91.
- [18] Nezamzadeh-Ejhieh, A., Khorsandi, S. (2014). Photocatalytic degradation of 4-nitrophenol with ZnO supported nano-clinoptilolite zeolite. *Journal of industrial and engineering chemistry*, 20(3), 937-946.
- [19] Cheng, H. H., Hsieh, C. C., Tsai, C. H. (2012). Antibacterial and regenerated characteristics of Ag-zeolite for removing bioaerosols in indoor environment. *Aerosol and air quality research*, 12(3), 409-419.
- [20] Zhong, S., Zhang, F., Yu, B., Zhao, P., Jia, L., Zhang, S. (2016). Synthesis of PVP-Bi₂ WO₆ photocatalyst and degradation of tetracycline hydrochloride under visible light. *Journal of materials science: Materials in electronics*, 27(3), 3011-3020.
- [21] Ghorai, T. K., Biswas, N. (2013). Photodegradation of rhodamine 6G in aqueous solution via SrCrO₄ and TiO₂ nano-sphere mixed oxides. *Journal of materials research and technology*, 2(1), 10-17.
- [22] Saadati, F., Keramati, N., Ghazi, M. M. (2016). Influence of parameters on the photocatalytic degradation of tetracycline in wastewater: a review. *Critical reviews in environmental science and technology*, 46(8), 757-782.
- [23] Keramati, N., Nasernejad, B., Fallah, N. (2014). Synthesis of N-TiO₂: stability and visible light activity for aqueous styrene degradation. *Journal of dispersion science and technology*, 35(10), 1476-1482.
- [24] Nakaoka, Y., Katsumata, H., Kaneco, S., Suzuki, T., Ohta, K. (2010). Photocatalytic degradation of diazinon in aqueous solution by platinized TiO₂. *Desalination and water treatment*, 13(1-3), 427-436.
- [25] Martínez, C. M. C. L., Fernández, M. I., Santaballa, J. A., Faria, J. (2011). Kinetics and mechanism of aqueous degradation of carbamazepine by heterogeneous photocatalysis using nanocrystalline TiO₂, ZnO and multi-walled carbon nanotubes-anatase composites. *Applied catalysis B: Environmental*, 102(3-4), 563-571.
- [26] Lin, H. Y., Shih, C. Y. (2012). Efficient one-pot microwave-assisted hydrothermal synthesis of Nitrogen-doped TiO₂ for hydrogen production by photocatalytic water splitting. *catalysis surveys from Asia*, 16(4), 231-239.
- [27] Daneshvar, N., Aber, S., Dorraji, M. S., Khataee, A. R., Rasoulifard, M. H. (2007). Photocatalytic degradation of the insecticide diazinon in the presence of prepared nanocrystalline ZnO powders under irradiation of UV-C light. *Separation and purification technology*, 58(1), 91-98.
- [28] Gaya, U. I., Abdullah, A. H. (2008). Heterogeneous photocatalytic degradation of organic contaminants over titanium dioxide: a review of fundamentals, progress and problems. *Journal of photochemistry and photobiology C: Photochemistry reviews*, 9(1), 1-12.
- [29] Sakkas, V. A., Calza, P., Vlachou, A. D., Medana, C., Minero, C., Albanis, T. (2011). Photocatalytic transformation of flufenacet over TiO₂ aqueous suspensions: Identification of intermediates and the mechanism involved. *Applied catalysis B: Environmental*, 110, 238-250.